Modeling of the Simultaneous Influence of the Thermal Noise and the Phase Noise in Space Communication Systems

Ondřej BARAN, Miroslav KASAL

Dept. of Radio Electronics, Brno University of Technology, Purkyňova 118, 612 00 Brno, Czech Republic

xbaran03@stud.feec.vutbr.cz, kasal@feec.vutbr.cz

Abstract. *Our work deals with studies of a noise behavior in space communication systems. Two most important noise types, the additive thermal noise and the multiplicative phase noise, respectively, are included. A simple model of the narrowband communication system is created and simulated in the Ansoft Designer system simulator. The additive thermal noise is modeled as AWGN in a communication channel. The phase noise is produced in transmitter and receiver oscillators. The main intention is to investigate the receiver filter bandwidth decrease effect on powers of both noise types. Results proposed in this paper show that for defined system conditions and for a certain filter bandwidth value, the power of the multiplicative phase noise equals to the additive thermal noise power. Another decrease of the filter bandwidth causes the phase noise power exceeding. To demonstrate the noise behavior transparently, input system parameters are properly selected. All simulation results are documented by theoretical calculations. Simulation outcomes express a good coincidence with presumptions and calculations.*

Keywords

Ansoft Designer, thermal noise, AWGN, phase noise, FIR filter, noise bandwidth.

1. Introduction

Generally, every communication system consists of three basic parts, a transmitter, a receiver and the useful information is transferred through a transmission channel. Each part has its negative features which influence and/or disturb the transmitted useful signal in a certain way. These negative features are very often in a contrary with high user demands for such a communication system. In the area of space communication systems, conditions are even more critical than in terrestrial systems. Very long communication distances, moving objects connected with the Doppler frequency shift effect and a noise belong to the most severe disturbing factors in a communication with space objects. In the wideband systems, the main noise type considered during the design is an additive thermal noise projected from the communication channel and from the receiver part. The narrowband low rate communication [1], e. g. with deep space probes, is in addition affected by the multiplicative phase noise, which arises from all oscillators in the whole communication system. The long distance causes huge signal attenuation during the free space transmission and system noise parameters are then very critical to the system quality. On the other hand, in space communications, a ground receiver antenna is pointed to the cold sky, thus the appropriate noise temperature of the communication channel is quite low. This leads to a fact that the influence of the phase noise increases and it can't be neglected.

The simultaneous incidence of both noise types on the system signal to noise ratio is an object of the investigation. The decreasing bandwidth of the receiver filter restricts the influence of the additive thermal noise and SNR is increasing. The same procedure is made with the multiplicative phase noise and the effect is observed.

2. Theoretical Description of the Communication System Model

In spite of a fact that transmitters and receivers are very complex subsystems, their simpler forms are used for the modeling and for the investigation of the noise influence. Obtained results have general validity. The proposed model can be extended and the previous results can be applied for that extension.

2.1 Basic Parameters Declaration

The model is created in Ansoft Designer system simulator and Fig. 1 depicts its look. All signals used in the simulated system have to be properly sampled according to the sampling theorem [2]. The sampling frequency is denoted as f_{sam}.

For a simplification, the useful baseband signal, denoted as $x(t)$, is a harmonic cosine wave. Its time domain form is described by the equation

$$x(t) = \frac{A}{2}\left(e^{j\omega_x t} + e^{-j\omega_x t}\right) \qquad (1)$$

where A is an amplitude and ω_x is an instantaneous angular frequency. To comply with the sampling theorem [2], the inequality $\omega_x \leq 2 \cdot (2\pi \cdot f_{sam})$ needs to be fulfilled.
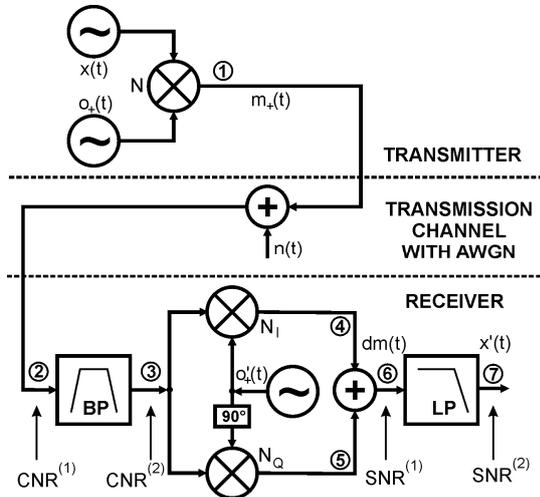
Fig. 1. A block diagram of the modeled communication system.

For a useful signal modulation, a carrier from a local oscillator is used. Its signal is described in the time domain as

$$o(t) = O \cdot \cos(\omega_O t + \Phi_O + \psi(t)) \qquad (2)$$

where O is the oscillator amplitude, ω_O is the instantaneous angular frequency, Φ_O is the initial phase and parameter $\psi(t)$ denotes time domain phase fluctuations (it is the expression of the frequency domain oscillator phase noise). It is supposed that oscillators have the amplitude limitation ability. Thus in a comparison with phase fluctuations, oscillator amplitude fluctuations can be neglected [3]. The frequency ω_O can reach about several orders higher values then the frequency of the useful modulating signal ω_x. To fulfill the sampling theorem for the oscillator signal $o(t)$, the sampling frequency f_{sam} has to be at least twice as high as the frequency f_O (f_O is the carrier instantaneous frequency, $\omega_O = 2\pi \cdot f_O$). In addition, to cover the statistical behavior of the noise, one needs a huge number of samples to process. This puts very severe claims for the computer power and the memory. To overcome this problem, the sampling of a passband signal as a baseband signal is used. The oscillator passband signal $o(t)$ is expressed as an analytic signal [2], [4] $o_+(t)$ with a one-sided spectrum according to

$$o_+(t) = O \cdot e^{j\psi(t)} \cdot e^{j\Phi_O} \cdot e^{j\omega_O t}. \qquad (3)$$

The first three terms of (3) refer to a complex envelope [4] that, in fact, represents the baseband signal which can be sampled by the sampling frequency f_{sam}. The complex sinusoid $\exp(j\omega_O t)$ causes the frequency transposition of the complex envelope to the vicinity around the carrier frequency ω_O.

For a demodulation, the analytic signal of the local oscillator has a form

$$o'_+(t) = O' \cdot e^{j\psi'(t)} \cdot e^{j\Phi_O} \cdot e^{-j\omega'_O t} \qquad (4)$$

where O' is the signal amplitude, ω'_O is the angular frequency, Φ'_O is the initial phase and $\psi'(t)$ represents time domain phase fluctuations. For the proper demodulation, frequencies and initial phases of transmitter and receiver oscillator signals have to be the same ($\omega_O = \omega'_O$ and $\Phi_O = \Phi'_O$). This condition is supposed to be accomplished in the whole text. For the simplification in the following text, the initial phase of transmitter and receiver oscillators is considered to be zero radians ($\Phi_O = \Phi'_O = 0$ rad).

Ansoft Designer simulator works with analytic signal representations, thus, derivations, used further in the text, also utilize this representation. Analytic signals are always denoted with symbol + in a lower index.

2.2 Additive Thermal Noise Modeling

The additive thermal noise is composed of the thermal noise of all blocks on the receiver side of the system (transmission channel as well as the single receiver). In this text, it is supposed that the overall additive thermal noise is re-calculated to the input of the receiver antenna [5], [6]. Thus, it is expressed as the transmission channel additive thermal noise.

The transmission channel is modeled as a sum-block which performs the sample-by-sample summation of the modulated signal $m_+(t)$ and the noise signal $n(t)$. The noise signal $n(t)$ has the normal Gaussian distribution with a zero mean and a variance σ^2_{AWGN}, that is directly equal to a noise power N. The channel modeled in such a way is denoted as AWGN (Additive White Gaussian Noise) channel [7]. The whole system model works with complex signals, thus, even the noise signal has to be complex

$$n(t) = n_I(t) + j \cdot n_Q(t). \qquad (5)$$

Both, the real part noise and the imaginary part noise, are independent non-correlated processes.

Originally, the signal $n(t)$ is represented in a baseband and is sampled by f_{sam}. After the noise signal $n(t)$ transposition to the passband (to the vicinity around the carrier f_O), a thermal noise power spectral density N_0 can be expressed as

$$N_0 = \frac{N}{f_{sam}} = \frac{\sigma^2_{AWGN}}{f_{sam}}. \qquad (6)$$
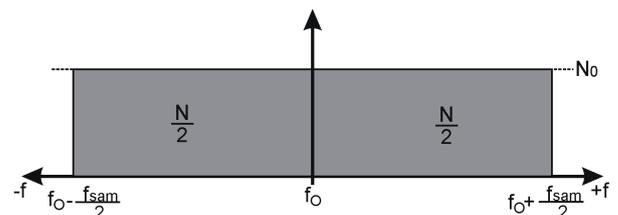
Fig. 2. Noise power spectral density derivation.

The noise power N is obtained as a sum of real and imaginary parts powers. One supposes a one-sided spectrum representation [8] and the situation is demonstrated by Fig. 2.

2.3 Multiplicative Phase Noise Modeling

Carrier waves are produced in oscillator models which can also simulate a phase noise behavior. The single sideband (SSB) phase noise denotes the frequency domain representation of time domain phase fluctuations (e.g. $\psi(t)$ from (3)). Ansoft Designer models the SSB phase noise $L(f_m)$ according to the Leeson formula [3]

$$L(f_m) = 10 \cdot \log\left\{\left(1 + \frac{f_c}{f_m} + \frac{f_{LO}^2}{(2q_{load}f_m)^2} + \frac{f_c f_{LO}^2}{(2q_{load})^2 f_m^3}\right)\frac{FkT}{2P_{LO}}\right\} \quad (7)$$

where f_m is the offset frequency from the carrier f_{LO}, f_c denotes the flicker noise corner frequency [3]. The oscillator power is P_{LO}, q_{load} refers to the loaded quality factor of the oscillator resonator and F denotes a noise figure of the oscillator active element. k is the Boltzman constant, T is the thermodynamic temperature of the oscillator ($k = 1.38 \cdot 10^{-23}$ JK^{-1}, usually $T = 290$ K).

The Leeson formula divides the frequency domain SSB phase noise course into 4 areas (see equation (7)). Each area corresponds to the individual phase noise type (see Tab. 1) [6], [9]. From Tab. 1, β denotes the slope of the individual phase noise type after a linear approximation of $L(f_m)$ in a log-log plot. It also expresses the power of a $L(f_m)$ decomposition into a power series.

phase noise type	β
white PM noise	0
flicker PM noise	−1
white FM noise	−2
flicker FM noise	−3

Tab. 1. Phase noise types covered by the Leeson formula [6].

2.4 Theoretical Derivations

The following subsections provide theoretical derivations of time domain signals and their powers in significant points of the system model (designations agree with Fig. 1).

Transmitter – *point 1*

According to Fig. 1, the transmitter contains only a DSB-SC modulator. The modulator is modeled as a complex multiplier that multiplies the modulating signal $x(t)$ with the carrier $o_+(t)$. The result is a modulated signal $m_+(t)$ and its time domain representation follows the equation

$$m_+(t) = x(t) \cdot o_+(t) =$$
$$= \frac{AO}{2}(1 + j\psi(t))\left(e^{j(\omega_O + \omega_x)t} + e^{j(\omega_O - \omega_x)t}\right). \quad (8)$$

After subtracting the signal $m_+(t)$ (8) from the ideal modulated signal (with a zero noise term $\psi(t)$), only the noise signal with the power $N_{(1)}$ is obtained

$$N_{(1)} = P\{\psi(t)\}\frac{(AO)^2}{2}. \quad (9)$$

This result implies from the fact that powers of a complex sine wave or a complex cosine wave are equal to the unity.

Transmission channel – *point 2*

The lossless transmission channel is modeled according to the earlier description. The additive thermal noise (simulated as AWGN) is added to the modulated signal $m_+(t)$ (8) and the result is $n(t) + m_+(t)$. The noise power $N_{(2)}$ observed in the *point 2* is equal to

$$N_{(2)} = P\{n(t)\} + P\{\psi(t)\}\frac{(AO)^2}{2}. \quad (10)$$

Receiver – passband part – *point 3*

A received signal passes through the band-pass filter BP. It is considered that the filter doesn't affect the useful signal, but it influences the noise of both types. Let one denote noise signals passed through the filter as $n(t) \rightarrow n_{BP}(t)$ and $\psi(t) \rightarrow \psi_{BP}(t)$. With these considerations, equation (10) can be rewritten to the form

$$N_{(3)} = P\{n_{BP}(t)\} + P\{\psi_{BP}(t)\}\frac{(AO)^2}{2}. \quad (11)$$

Now, the question is, how exactly the band-pass filter affects the additive noise and the phase noise. For each filter, its noise bandwidth BN_{BP} can be calculated with a help of a filter's power transfer function [5], [10]. When the filter is high order, the steepness of its transfer function is very high and the filter noise bandwidth can be considered to be equal to the filter 3 dB bandwidth.

The usage of analytic signals and complex envelopes brings a certain simplification into the filtering. Instead of a band-pass filter, the low-pass filtering is used [4]. In a classical conception, the band-pass filter influence on the additive noise can be explained according to the Fig. 3.
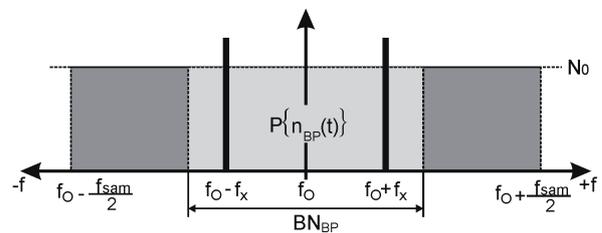
Fig. 3. A derivation of the additive noise power after band-pass filtration.

A complex analytic signals conception enables shifting the signal to the baseband, where the noise bandwidth of the equivalent low-pass filter is $BN_{BP}/2$. If the additive noise power spectral density N_0 is known (see (6)), then the additive noise power after filtration equals to [5]

$$P\{n_{BP}(t)\} = 2 \cdot N_0 \cdot \frac{BN_{BP}}{2} = N_0 \cdot BN_{BP}. \qquad (12)$$

The factor 2 denotes the reality that, in fact, one works with both lower and upper frequency components after the modulation (the situation is in accordance with Fig. 3).

In a case of the multiplicative phase noise, the filtration problem is more complicated. The situation is demonstrated in Fig. 4. At the beginning, one expects a high steepness of the filter transfer function, thus, the concept of the noise bandwidth can be used. Behind the filter passband, noise sidebands are considered to be suppressed so well that they can be neglected. Fig. 4 demonstrates the real situation, while in simulations, the concept of analytic signals and the passband signal shifting to the baseband is utilized (indeed, with same results). The low-pass filter is used instead of the band-pass one (in the same way as in the previous case with the additive noise).
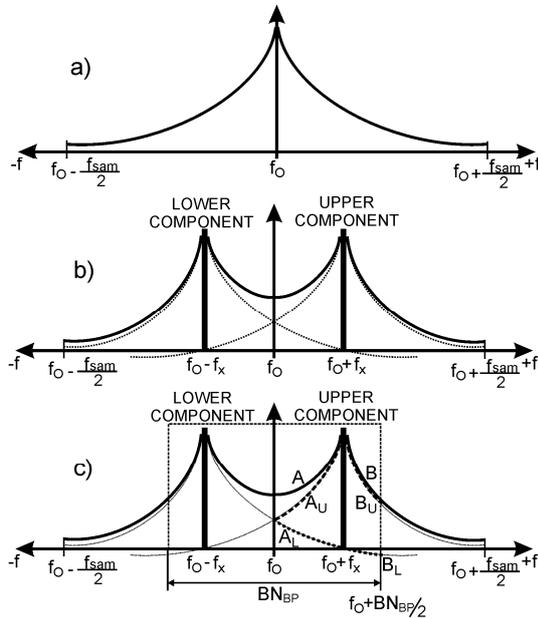
Fig. 4. The modulation and filtration influence on the phase noise, a) carrier phase noise sidebands, b) a transformation of the phase noise after the modulation, c) a principle of the filtered phase noise calculation after the modulation.

Phase noise sidebands in the vicinity of the carrier (e.g. $o_+(t)$) are demonstrated in Fig. 4 a). The phase noise power in one sideband (upper or lower) can be calculated as a numerical integration of the SSB phase noise course $L(f_m)$

$$P\{PN_{carr}\} = \int_{f_1}^{f_2} L(f_m) df_m \qquad (13)$$

where f_1 and f_2 are integral limits. In a case of the carrier phase noise, the limits are following $f_1 = \Delta f$ and $f_2 = f_{sam}/2$. The low limit frequency f_1 is not allowed being zero (the phase noise doesn't cover the carrier), thus, the parameter Δf represents the offset step from the carrier. The total carrier phase noise power is two times the power calculated

according to (13) (the upper sideband power plus the lower sideband power).

After the modulation, the situation with phase noise changes as can be seen in Fig. 4 b). The upper component (vicinity of $f_O + f_x$) and the lower component (vicinity of $f_O - f_x$) are created. The phase noise power of each component independently is a half compared to the carrier phase noise power (integrated according to thin doted lines around each component in Fig. 4 b)). The total modulated phase noise power equals to a summation of upper noise component and lower noise component contributors (in other words, the proper integration according to the thick solid line in Fig. 4 b) has to be done). The result directly corresponds to the carrier phase noise power.

To calculate the phase noise power after the filtration, the following solution is proposed. One focuses only to the upper component of the modulated signal, where the problem is divided in to the lower part A and the upper part B (see Fig. 4. c)). In each part, the integration

$$P\{PN_{mod}\} = \frac{1}{2} \int_{f_1}^{f_2} L(f_m) df_m \qquad (14)$$

is utilized. A lower index *mod* is in turn replaced by a particular part (A_U, A_L, B_U, B_L; see Fig. 4 c)) in which limits f_1 and f_2 for integration of $L(f_m)$ differ.

The upper part B is created by the upper phase noise sideband B_U of the upper component (a thick dashed curve in Fig. 4 c)) and by the upper phase noise sideband B_L of the lower component (a thick doted curve in Fig. 4 c)). Then for the B_U part, the limits are $f_1 = \Delta f$ and $f_2 = BN_{BP}/2 - f_x$. The limits for the B_L part are $f_1 = 2 \cdot f_x + \Delta f$ and $f_2 = BN_{BP}/2 + f_x$. The lower part A is shaped by the lower phase noise sideband A_U of the upper component (a thick dashed curve in Fig. 4 c)) and by the upper phase noise sideband A_L of the lower component (a thick doted curve in Fig. 4 c)). Then, the limits for A_U part are $f_1 = \Delta f$ and $f_2 = f_x$ (it implies from the flipped course of $L(f_m)$). The limits for the A_L part are $f_1 = f_x$ and $f_2 = 2 \cdot f_x - \Delta f$.

According to the previous procedure, after integral (14) calculations, one obtains four partial noise powers. The total noise power of one component is a sum of these four partial noise powers

$$P\{PN_{mod\_1comp}\} = $$
$$= P\{PN_{B_U}\} + P\{PN_{B_L}\} +$$
$$+ P\{PN_{A_U}\} + P\{PN_{A_L}\} =$$
$$= \frac{1}{2}\left[\int_{\Delta f}^{BN_{BP}/2-f_x} L(f_m) df_m + \int_{2 \cdot f_x}^{BN_{BP}/2+f_x} L(f_m) df_m + \right.$$
$$\left. + \int_{\Delta f}^{f_x} L(f_m) df_m + \int_{f_x}^{2 \cdot f_x - \Delta f} L(f_m) df_m \right]. \qquad (15)$$

Doubling this total noise power, the overall phase noise power $P\{\psi_{BP}(t)\}$ in the modulated signal is gained (upper

and lower components have identical power and are symmetrical around the carrier frequency, $P\{\psi_{BP}(t)\}=2P\{PN_{mod\_1comp}\}$).

With a lower filter order, the filter transfer function steepness decreases and the above procedure gives less accurate results. Again, one has four parts (A_U, A_L, B_U, B_L) to be integrated and their sum forms the total noise power of each component. But in this case, for parts B_U and B_L, in the frequency domain, the SSB phase noise course $L(f_m)$ needs to be multiplied by a real filter transfer function shifted to the right position on the frequency axis. For both parts, the integration limits changes to the following: for B_U $f_1 = \Delta f$ and $f_2 = f_{sam}/2$, for B_L $f_1 = 2 \cdot f_x$ and $f_2 = f_{sam}/2$. The process for the calculation of powers of parts A_U and A_L stays the same as above. The overall modulated phase noise power is also the double of the component noise power.

Receiver – baseband part – *point 6*

A demodulation is implemented by a help of a quadrature system [8]. The quadrature demodulator consists of two complex multipliers that are fed by the received filtered signal on the first input and by the local oscillator signal on the second input. The in-phase multiplier N_I is driven directly by the oscillator signal $o'_{+I}(t) = o'_{+}(t)$. The quadrature multiplier N_Q is controlled by the oscillator signal that is phase shifted about 90°

$$o'_{+Q}(t) = o'_{+}(t) \cdot e^{j\pi/2}. \qquad (16)$$

The sum of in-phase and quadrature products gives the complex analytic demodulated signal $dm_{+}(t)$. For the demodulation back to the baseband, frequencies of modulator and demodulator oscillators are the same, $\omega_O = \omega'_O$. When this condition is fulfilled, Ansoft Designer takes only the real part of the quadrature demodulator output signal

$$\begin{aligned}
dm(t) &= \mathrm{Re}\{dm_{+}(t)\} = \\
&= n_{BPI}(t)O'[\cos(\omega'_O t) + \sin(\omega'_O t) + \\
&\quad + \psi'(t)(-\cos(\omega'_O t) + \sin(\omega'_O t))] - \\
&\quad - n_{BPQ}(t)O'[\cos(\omega'_O t) - \sin(\omega'_O t) + \\
&\quad + \psi'(t)(\cos(\omega'_O t) + \sin(\omega'_O t))] + \\
&\quad + [1 - (\psi_{BP}(t) + \psi'(t))]AOO'\cos(\omega_x t).
\end{aligned} \qquad (17)$$

In the demodulated signal, both parts (in-phase and quadrature) of the complex additive noise are presented. After the same presumptions as in other points of the system, subtracting the distorted demodulated signal (17) from the ideal one (zero terms $n_{BP}(t) = 0$, $\psi_{BP}(t) = 0$ and $\psi'(t) = 0$), the single noise signal is obtained. Its power equals to

$$\begin{aligned}
N_{(6)} &= O'^2 P\{n_{BP}(t)\} + O'^2 P\{n_{BP}(t)\}P\{\psi'(t)\} + \\
&\quad + [P\{\psi_{BP}(t)\} + P\{\psi'(t)\}]\frac{(AOO')^2}{2}.
\end{aligned} \qquad (18)$$

The power of the demodulator oscillator phase noise $P\{\psi'(t)\}$ is gained as a double of the integration according to (13) with the following limits $f_1 = \Delta f$ and $f_2 = f_{sam}/2$.

Receiver – final signal – *point 7*

The final step to get the demodulated signal $x'(t)$ in the baseband is the low-pass LP filtration of the signal $dm(t)$ (17). The main assumption is that the LP filter doesn't affect the useful signal. The LP influences only the amount of the noise power, thus, time domain noise signals can be rewritten as $n_{BP}(t) \rightarrow n_{LP}(t)$, $\psi_{BP}(t) \rightarrow \psi_{LP}(t)$ and $\psi'(t) \rightarrow \psi'_{LP}(t)$. With these conditions, the noise power can be obtained after a simple modification of equation (18) to the form

$$\begin{aligned}
N_{(7)} &= O'^2 P\{n_{LP}(t)\} + O'^2 P\{n_{LP}(t)\}P\{\psi'_{LP}(t)\} + \\
&\quad + [P\{\psi_{LP}(t)\} + P\{\psi'_{LP}(t)\}]\frac{(AOO')^2}{2}.
\end{aligned} \qquad (19)$$

The same question here is, how exactly the low-pass filter affect the additive noise and the multiplicative phase noise and how the power of such a filtered noise can be calculated. Similarly as above, the low-pass filter noise bandwidth BN_{LP} can be calculated [5], [10]. The high filter order secures a sufficient steepness of the filter transfer function which also allows using the noise bandwidth concept for the phase noise. Let one make another assumption, the low-pass filter bandwidth is always equal to or less than the half of the band-pass filter bandwidth. The reason will emerge from the following paragraphs and pictures.

In a case of the additive noise, the procedure depicted in Fig. 5 can be utilized (a similar way as for the band-pass filter earlier [8]). When the noise power spectral density N_0 is known (7), then, after substituting BN_{LP} instead of BN_{BP} into (12), the following formula can be used

$$P\{n_{LP}(t)\} = 2 \cdot N_0 \cdot BN_{LP}. \qquad (20)$$

Factor 2 denotes the two-sided spectrum division of the power between positive and negative frequencies.
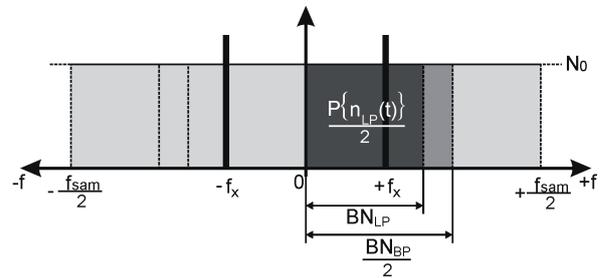
Fig. 5. An expression of the additive noise power after a low-pass filtration.

For the phase noise, the influence of the low-pass filtration can be also described similarly as for the band-pass filter case. The whole procedure stays the same, just BN_{LP} is substituted for $BN_{BP}/2$. Calculations are made twice, once for the transformed modulator oscillator phase noise $\psi_{BP}(t)$, and the second time for the demodulator oscillator

phase noise $\psi'(t)$. The same rules as for the BP filter holds for the decreasing steepness of the LP filter. The results are used in calculations according to (19).

In a case of high order filters with a high steepness of their transfer function, if $BN_{BP}/2 < BN_{LP}$, noise contributors $n_{BP}(t)$ and $\psi_{BP}(t)$ are considered not to be affected by the LP filter. Only the phase noise of the demodulator oscillator is influenced. On the other hand, when the filter steepness decreases, the real filters transfer functions have to be used for the filtration of the phase noise courses.

3. Model Settings in Ansoft Designer

The system model according to Fig. 1 can be created in different simulating programs. Each of them has its specific demands that need to be kept to obtain correct results. The following paragraphs sum up important features and parameters that have to be coped with in Ansoft Designer simulator.

The minimal offset frequency of the generated phase noise in Ansoft Designer is 100 Hz from the carrier. This restriction is established in the parameter Δf, that is used in the previous equations. The space between the carrier and the limit 100 Hz is created by the distortion implying from the imperfect signal sampling. This fact has to be considered in theoretical calculations to a proper comparison with simulation results. Upper sideband frequency spectrum details of the modulator oscillator with and without the phase noise are demonstrated in Fig. 6.

Both BP filters and a LP filter are realized by the FIR low-pass filters. The received signal before the BP filter (*point 2*, see Fig. 1) is complex. To perform the FIR filtration, this complex signal is divided into its real and imaginary parts that are filtered separately. The resulting parts are combined back to the complex signal (*point 3*). The demodulated signal (*point 6*) is just real, thus, this modification isn't necessary.
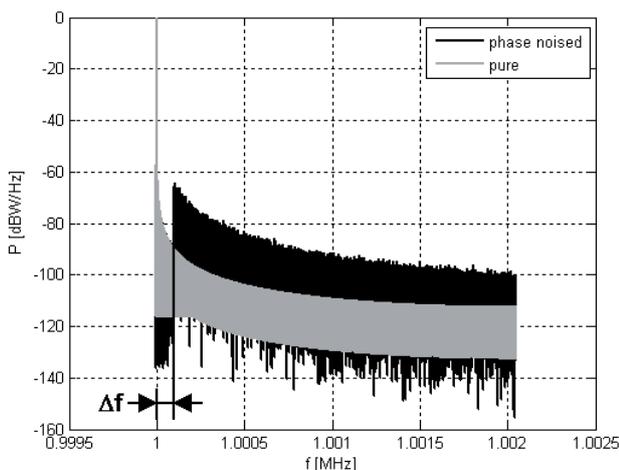
Fig. 6. A comparison of frequency spectra of the oscillator signal $o_+(t)$ with and without the phase noise.

In reality, the modeled quadrature demodulator contains two separate oscillators. Their signals are set to be 90° phase shifted. This solution has an advantage in a contrary to a realization with one oscillator and a phase shifter. The phase shifter can be realized by a delay block that delays the incoming signal about a certain number of samples. The problem is that the integer number of samples can't cover exactly the phase shift 90° and emerging deviations can increase errors.

Every noise generating block has a parameter seed, which is used for the random number generator. For each block, the seed parameter has to be set differently to obtain the uncorrelated independent noise signals. The exception is in a case of the quadrature demodulator, where both oscillators must have equal seed parameters (in fact, they express one oscillator with two phase shifted output signals with the same phase noise distortion).

4. Simulation Results and Comparison

The basic communication system model according to Fig. 1 is created in Ansoft Designer simulator. The chain model is made in two parallel branches. One represents a reference ideal system without any noise source. The second branch is, in turn, degraded by an additive noise, then by a multiplicative phase noise and finally, by both noise types simultaneously. This organization allows one to measure signal to noise ratios between ideal and distorted branches in the simulator (in *points 2* and *3* $CNR^{(1)}$ and $CNR^{(2)}$, in *points 6* and *7* $SNR^{(1)}$ and $SNR^{(2)}$, see Fig. 1). Signal to noise ratios are used for noise powers derivations. Simulation results are compared with theoretical calculations processed in Matlab (programmed according to derivations in chapter 2). Parameters used during simulations are chosen properly to provide transparent results.

Concrete settings of the system model

Basic parameters that have to be set in signal sources models are summarized in Tab. 2. The sampling frequency in the whole simulation is chosen to $f_{sam} = 4096$ Hz.

quantity name	value	unit
Modulating signal $x(t)$		
amplitude A	$\sqrt{2}$	V
power P$\{x(t)\}$ *	1	W
frequency f_x	150	Hz
Modulator carrier $o(t)$		
amplitude O	1	V
power P$\{o_+(t)\}$ *	1	W
frequency f_O	1	MHz
PN power P$\{\psi(t)\}$ *	-32,678	dBW
Demodulator carrier $o'(t)$		
amplitude O'	1	V
power P$\{o'_+(t)\}$ *	1	W
frequency f'_O	1	MHz
PN power P$\{\psi'(t)\}$ *	-36,735	dBW

* powers are calculated over 1 Ω resistance

Tab. 2. Settings of signal sources parameters.

The frequency domain phase noise courses corresponding to modulator oscillator phase fluctuations $\psi(t)$ and to demodulator oscillator phase fluctuations $\psi'(t)$ are shown in Fig. 7. Simulation results are compared with calculations according to (7).
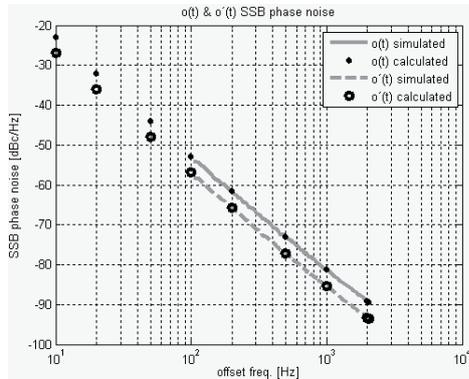
Fig. 7. Simulated and calculated frequency domain SSB phase noise courses.

Ansoft Designer simulator enables the direct connection of a complex AWGN channel. The main parameter characterizing the amount of added noise is the signal to noise ratio *SNR*. The AWGN channel model measures the power of the input useful signal and, according to *SNR*, it generates the noise signal $n(t)$ with the power N (equations (5) and (6)). The AWGN block output is the signal degraded by an additive noise. The parameter *SNR* is set to $SNR = 27$ dB.

filter designation	3 dB bandwidth	noise bandwidth BN_{BP}	noise bandwidth $BN_{BP}/2$ *
	Hz	Hz	Hz
band-pass filters			
BP1	320	321,19	160,59
BP2	360	361,15	180,57
BP3	420	421,18	210,59
BP4	500	501,18	250,59
BP5	600	601,19	300,59
BP6	800	801,17	400,58
BP7	1000	1001,20	500,60
BP8	1300	1301,18	650,58
BP9	1500	1501,17	750,59
BP10	1700	1701,17	850,58
BP11	2000	2001,20	1000,60
low-pass filter			
		BN_{LP}	BN_{LP}
LP1	160	160,59	160,59

* the noise bandwidth of an equivalent low-pass filter expression used for a band-pass filters simulation

Tab. 3. A characterization of FIR filters used in simulations.

In a passband part (between *points 2* and *3*, in Fig. 1), for a filtration, a bank of band-pass BP filters is created. As was written in section 3, they are composed as low-pass FIR filters. Filters are characterized by a vector of filter coefficients [2]. The advantage of FIR filters usage is a constant group delay and a faster simulation processing. Their disadvantage is a need of high filter order to reach for the sharp steepness of the filter transfer function. For a final signal filtration (between *points 6* and *7*, in Fig. 1),

a low-pass FIR filter is used. The order of all filters in the system model is set to 1000. Bandwidths of individual filters calculated according to [5], [10] are summarized in Tab. 3.

The following paragraphs summarize simulation results compared with theoretical presumptions and calculations. The main concern is devoted to the investigation of the filter bandwidth reduction influence on the noise behavior. Results are expressed graphically. X axis shows the noise bandwidth change and y axis represents the noise power (in dBW).

Transmission channel – *point 2*

In this point of the system model, no filters are used so far. There is no noise dependency on the filter bandwidth. After substituting of all quantities from Tab. 3 into equation (10), theoretical noise powers are obtained (see Tab. 4). (An abbreviation PN means the phase noise.)

	noise power $N_{(2)}$		
noise type	AWGN only	PN only	AWGN & PN
unit	dBW	dBW	dBW
theory	-26,993	-32,649	-25,949
simulations	-26,993	-32,652	-25,950
conditions	$\psi(t) = 0$	$n(t) = 0$	$\psi(t) \neq 0$, $n(t) \neq 0$

Tab. 4. Theoretical versus simulation results in *point 2*.

Receiver – passband part – *point 3*

The first part of the receiver model (see Fig. 1) is the band-pass BP filter performing the noise reduction. After calculating the filter influence on both noise types (equations (11) - (15)), the noise power dependency on the noise bandwidth change is depicted in Fig. 8 (both theoretical and simulation results are covered). A numerical example for the filter BP1 is summarized in Tab. 5.
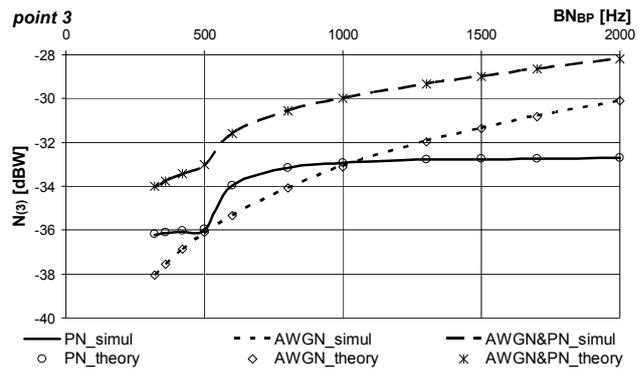
Fig. 8. The noise bandwidth influence on the noise power in the passband part of the system – *point 3*.

	noise power $N_{(3)}$		
noise type	AWGN only	PN only	AWGN & PN
unit	dBW	dBW	dBW
theory	-38,049	-36,180	-34,004
simulations	-38,056	-36,217	-34,033
conditions	$\psi(t) = 0$	$n(t) = 0$	$\psi(t) \neq 0$, $n(t) \neq 0$

Tab. 5. Theoretical versus simulation results in *point 3*, for a filter BP1.

Receiver – baseband part – *point 6*

The passband signal is demodulated to the baseband with a help of the demodulator oscillator that is distorted by the phase noise (proportional to phase fluctuations $\psi'(t)$). Using the description in section 2 (equations (12) - (15) and (18)), the noise power dependency on the noise bandwidth change is calculated. Comparisons between both theoretical and simulation results are shown in Fig. 9.
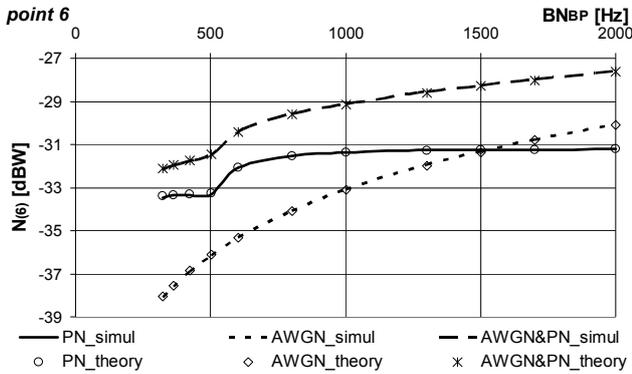
Fig. 9. The noise bandwidth influence on the noise power in the baseband part of the system – *point 6.*

Tab. 6 demonstrates differences between theoretical and simulation values on an example of the filter BP1.

noise type	noise power $N_{(6)}$		
	AWGN only	PN only	AWGN & PN
unit	dBW	dBW	dBW
theory	-38,049	-33,394	-32,115
simulations	-38,089	-33,480	-32,213
conditions	$\psi(t) = 0,$ $\psi'(t) = 0$	$n(t) = 0$	$\psi(t) \neq 0,$ $\psi'(t) \neq 0,$ $n(t) \neq 0$

Tab. 6. Theoretical versus simulation results in *point 6*, for a filter BP1.

Receiver – final signal – *point 7*

The final demodulated signal in the baseband is created after the LP filtration. The results calculated according to (19) and the simulation results implying from the low-pass filtration are depicted in Fig. 10.
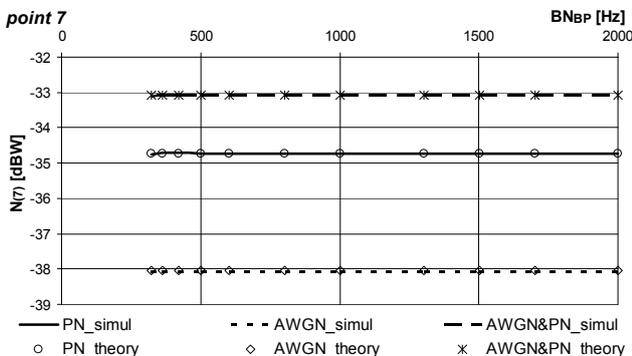
Fig. 10. The noise bandwidth influence on the noise power of the final demodulated signal – *point 7.*

When the low-pass filter noise bandwidth is equal to or is less than a half of the noise bandwidth of the band-pass filter, then the final noise curves are constant. This presumption is confirmed by simulations (see Fig. 10). The amount of the final noise is mostly given by a frequency band specified by the low-pass filter, no matter how the band-pass filter bandwidth is. Again, as an example, theoretical and simulation numerical values for the filter BP1 case are summarized in Tab. 7.

noise type	noise power $N_{(7)}$		
	AWGN only	PN only	AWGN & PN
unit	dBW	dBW	dBW
theory	-38,049	-34,739	-33,076
simulations	-38,095	-34,757	-33,131
conditions	$\psi(t) = 0,$ $\psi'(t) = 0$	$n(t) = 0$	$\psi(t) \neq 0,$ $\psi'(t) \neq 0,$ $n(t) \neq 0$

Tab. 7. Theoretical versus simulation results in *point 7*, for a filter BP1.

From previous graphical results, the filter bandwidth influence on the amount of the additive thermal noise and the multiplicative phase noise is obvious. Fig. 8 and Fig. 9 show the boundary of the filter noise bandwidth, when the power of the additive noise equals to the power of the phase noise. The amount of the additive noise power decreases linearly with the descending filter bandwidth (in Fig. 8 and Fig. 9, courses are not linear because of a logarithmic expression of power levels on y axis). The phase noise power decreases very slowly with the reducing filter bandwidth. In Fig. 8, for the received passband signal, the boundary filter bandwidth is approximately 1000 Hz. In the baseband, after the demodulation, this bandwidth boundary even increases to approximately 1500 Hz. The filter bandwidth reduction below these boundary bandwidths causes an increase of the phase noise power portion in the final noise power very expressively (over the additive noise power portion). If the useful harmonic signal frequency is $f_x = 150$ Hz, a half of the band-pass filter bandwidth can be e.g. $1.5 \cdot f_x$. According to simulation results, in this band, the multiplicative phase noise has much higher portion than the additive noise. In the final baseband signal, after the low-pass filtration, the phase noise influence predominates. Even if powers of the individual oscillators phase noise are much lower than the power of the channel additive noise, the final noise ratios are exactly opposite. The solution leading to improvements of system noise parameters lies in the reduction of the system oscillators phase noise.

A remark on Ansoft Designer phase noise results

As can be seen in Fig. 8 and Fig. 9, courses of the phase noise power show a quite sharp step down when decreasing the band-pass filter noise bandwidth. The sharp fall-down ends on the frequency approximately 500 Hz. This value implies from the following consideration. The Ansoft Designer phase noise generation is restricted by the minimal start offset frequency $\Delta f = 100$ Hz. Another fact is the modulating signal frequency $f_x = 150$ Hz. Summing this two values (on the one side of the modulated signal spectrum) and doubling the result (lower and upper frequency components), one obtains the desired value 500 Hz. This consideration is suggested in Fig. 11.
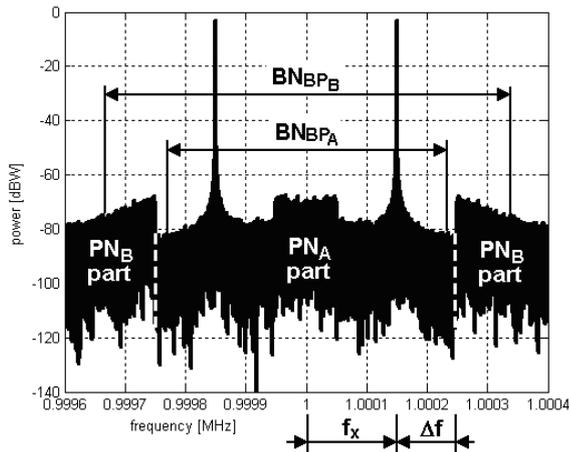
Fig. 11. An explanation of steps in phase noise power courses.

If a half of the filter noise bandwidth $BN_{BP}/2$ is less than the sum $\Delta f + f_x$, the phase noise power is almost the same (see Fig. 11, BN_{BPA}, only the noise part PN_A around modulated components is included). But after increasing $BN_{BP}/2$ over the sum $\Delta f + f_x$ (see Fig. 11, BN_{BPB}), the phase noise power abruptly increases because remaining phase noise sidebands (see Fig. 11, denoted as PN_B parts) start to be included. Theoretically, if Ansoft Designer hadn't the restriction, the course (in Fig. 8 and Fig. 9) of the phase noise power wouldn't decrease so rapidly, no sharp steps would be presented.

5. Conclusion

The research described in this paper shows the importance of the phase noise especially in space communication systems, where the narrowband communication with space probes is exploited. The simple communication system model is designed and the simultaneous effect of an additive thermal noise (simulated as AWGN in a communication channel) and a multiplicative phase noise of oscillators is observed, while the receiver filter bandwidth is being decreased. The main results give noise powers in important system points. The simulation is run three times, firstly only with the additive noise, then only with the phase noise and finally with an influence of both noise types. From the obtained noise powers, the filter bandwidth boundary, where powers of the additive noise and the phase noise are equal, can be found. Comparing the useful signal frequency with the filter bandwidth boundary, one can find out both the powers of both noise types and which noise type is predominating. The deep focus is devoted to descriptions of the phase noise and the additive noise after the filtration and the repeated filtration. The obtained simulation results are in a very good coincidence with presumptions and theoretical calculations that are made for all simulation cases.

The presented simple simulation procedure provides general conclusions that can be used in extended and much complicated models. In our future work, the current model will be extended. The input harmonic signal will be re-placed by the random bit generator and the simultaneous influence of both noise types on the demodulated signal BER will be observed. This model will simulate the BPSK narrowband low rate communication. Other extensions can include a mixing of modulated signals to microwave frequency bands, where the phase noise of other oscillators has to be counted in.

Acknowledgement

References

[1] ŠPAČEK, J., KASAL, M. The low rate telemetry transmission simulator. *Radioengineering*, 2007, vol. 16, no. 4, p. 24-31.

[2] PROAKIS, J. G. *Digital Communications* (4th Edition). New York: McGraw-Hill, 2001. p. 1024.

[3] LEE, T. H., HAJIMIRI, A. Oscillator phase noise: A tutorial. *IEEE Journal of Solid-State Circuits*, 2000, vol. 35, no. 3, p. 326 – 336.

[4] MEYR, H., MOENECLAEY, M., FECHTEL, S. A. *Digital Communication Receivers: Synchronization, Channel Estimation and Signal Processing*. New Jersey: John Willey & Sons, 1998.

[5] KASAL, M. *Radio Relay and Satellite Communication*. Lecture notes. Brno: MJ Servis, 2003. ISBN 80-214-2288-2. (In Czech.)

[6] BARAN, O., KASAL, M. Modeling of the phase noise in space communication systems. *Radioengineering*, 2010, vol. 19, no. 1, p. 141-148.

[7] VASILESCU, G. *Electronic Noise and Interfering Signals: Principals and Applications*. Berlin: Springer, 2005. 728 pages.

[8] ROBINS, W. P. *Phase Noise in Signal Sources*. London: Peter Peregrinus Ltd, 2007. ISBN: 987-0-86341-026-0.

[9] RILEY, J. *Handbook of Frequency Stability Analysis*. Beaufort: Hamilton Technical Services, 2007. [Online] Cited 2010-10-06. Available at: http://www.stable32.com/Handbook.pdf.

[10] CHANG, K. *Encyclopedia of RF and Microwave Engineering*. New Jersey: John Willey & Sons, 2005.

About Authors ...

Ondřej BARAN, Miroslav KASAL – for biography see *Radioengineering*, April 2010, vol. 19, no. 1, p. 148.